

Electronic Supplementary Information

Formation of Right-handed and Left-handed Chiral Nanopores within a Single Domain during Amino Acid Self-Assembly on Au(111)

Sena Yang,^a Aram Jeon,^a Russell W. Driver,^a Yeonwoo Kim,^a Eun Hee Jeon,^a Sehun Kim,^a Hee-Seung Lee*^a and Hangil Lee*^b

^aDepartment of Chemistry, Molecular-Level Interface Research Center, KAIST, Daejeon 305-701, Republic of Korea. E-mail: hee-seung_lee@kaist.ac.kr

^bDepartment of Chemistry, Sookmyung Women's University, Seoul 140-742, Republic of Korea. E-mail: easyscan@sookmyung.ac.kr

Table of Content

Experimental Section	S1
HRPES of 1 on the Au(111) Surface	S3
STM Images of Naphthalene on the Au(111) Surface	S4
HRPES of Naphthalene on the Au(111) Surface	S7
Proposed Structural Models for 1 and Naphthalene on the Au(111) surface	S8
References	S9

Experimental Section

Scanning tunneling microscopy

STM experiments were performed with an ultrahigh-vacuum system equipped with an OMICRON VT-STM instrument at a base pressure $< 1.0 \times 10^{-10}$ torr. Each Au(111) surface was cleaned by subjecting the substrate to several sputtering cycles of 0.5 keV Ar⁺ ions for 20 minutes followed by annealing at 700 K for 10 minutes; a clean surface image with a characteristic herringbone pattern was observed.

Compound **1** was synthesized according in four steps according to literature precedent.^{S1} Naphthalene (C₁₀H₈, 99% purity) was purchased from Sigma-Aldrich. Substrates were purified by turbo pumping for 30 minutes to remove impurities before dosing onto the Au(111) surface. A direct dozer controlled by a valve was used to introduce molecules. To obtain an appropriate vapor pressure for dosing, the covar was heated at 1.4 A, ~50 °C during source deposition. After exposing the molecules on the Au(111) surface at room temperature, the substrate was cooled to 150 K to minimize the surface mobility of molecules.

Density functional theory calculations

We performed the density functional theory (DFT) calculations to obtain geometry optimization and this single point energy of windmill-shaped tetramer and self-associated octamer of **1** in the absence of the Au(111) surface because we speculate that the interactions between **1** and Au(111) surface are almost never. All DFT energy calculations

were performed using the JAGUAR 9.1 software package, which applied a hybrid density functional method and included Becke's three-parameter nonlocal exchange functional with the correlation functional of Lee–Yang–Parr (B3LYP).^{S2} The geometries corresponding to the important local minima on the potential energy surface were determined at the basis set, B3LYP/6-31G** level of theory.^{S3-S4}

High Resolution Photoemission Spectroscopy

HRPES measurements were conducted at the 10D beamline of the Pohang Accelerator Laboratory. The Au 4*f*, C 1*s*, N 1*s*, and O 1*s* core-level spectra were obtained with a PHOIBOS 150 electron energy analyzer equipped with a two-dimensional charge-coupled device (2D CCD) detector (Specs GmbH). Photon energies of 140, 340, 450, and 580 eV were used to enhance the surface sensitivity. The binding energies of the three core-level spectra were calibrated with respect to that of the clean Au 4*f* core-level spectrum (84.0 eV) for the same photon energy. The base pressure of the chamber was maintained below 9.5×10^{-11} Torr. All spectra were recorded in the normal emission mode. The photoemission spectra were carefully analyzed by using a standard nonlinear least squares fitting procedure with Voigt functions.^{S5}

HRPES of **1** on the Au(111) Surface

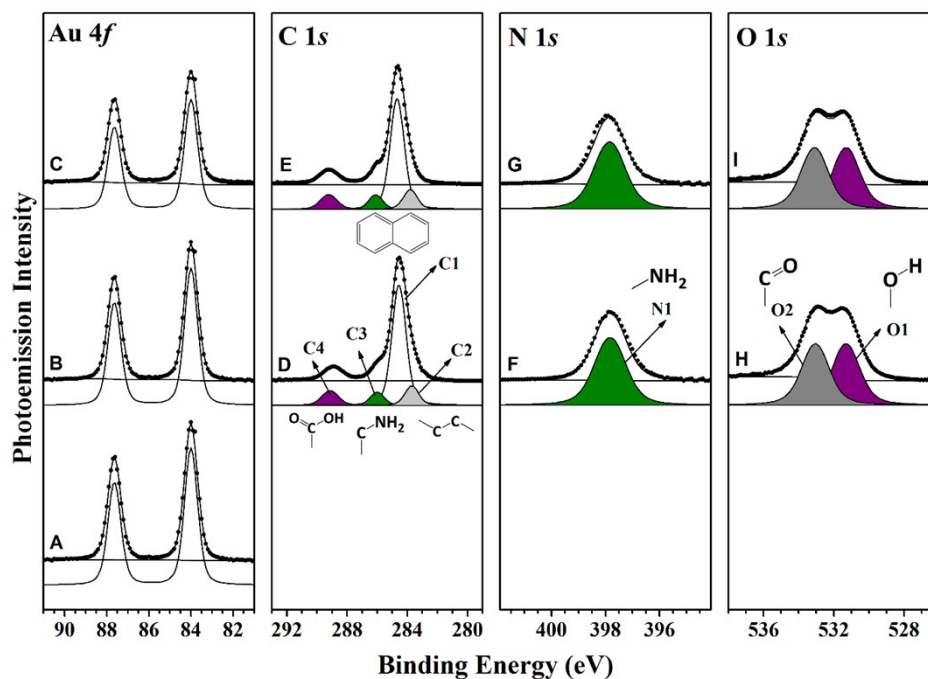


Fig. S1 The coverage-dependent core-level photoemission spectra of **1** on the Au(111) surface at low temperature. (b), (d), (f), and (h) represent Au 4f, C 1s, N 1s, and O 1s spectrum at low coverage, respectively. (c), (e), (g), and (i) represent Au 4f, C 1s, N 1s, and O 1s spectrum at high coverage, respectively.

We then obtained the C 1s core-level spectrum of **1** on the Au(111) surface. As shown in Fig. S1(d), this spectrum contains four distinct bonding features corresponding to the carbons of **1**. By considering the relationship between electronegativity and binding

energy, we assigned the bonding features C1, C2, C3, and C4 to aromatic carbon (284.21 eV), -C-C- (283.36 eV), C-NH₂ (285.72 eV), and COOH (288.67 eV), respectively.⁵⁶ As the deposition coverage increases, the binding energies of the four distinct bonding features are shifted slightly to higher energies (as shown in Fig. S1(e)).

There is only one feature in the N 1s core-level spectrum, at 397.8 eV, which is due to the amine group (-NH₂) of **1**.⁵⁷ As the coverage increases, the binding energy is shifted to high binding. The O 1s spectrum of **1** has two components due to O-H (O1, 530.79 eV) and C=O (O2, 532.55 eV). These indicate that amine group and carboxyl group do not have strong chemical bonds.

STM Images of Naphthalene on the Au(111) Surface

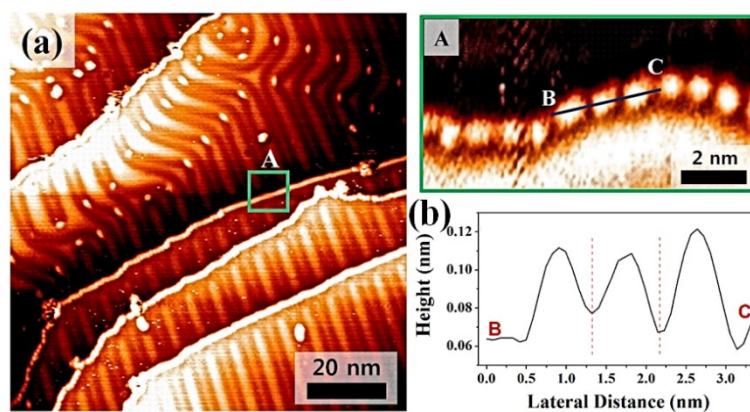


Fig. S2 Low coverage filled-state STM images of naphthalene on the Au(111) surface at 150 K: (a) 100.0 × 100.0 nm², V_s = −2.0 V, I_t = 0.1 nA, A) magnified STM image of (a), 10.0 × 5.0 nm², V_s = −2.0 V, I_t = 0.1 nA. (b) Line profile along the line BC in A.

To study the effects of functionalities in **1** on the formation on its self-assembled structures, we compared these results with those for naphthalene. After checking the cleanliness of the Au(111) surface, we deposited naphthalene molecules at 1.0×10^{-8} Torr for 3 minutes. This naphthalene deposition time is less than that for **1** because the naphthalene vapor pressure is higher than that of **1** by a factor of approximately 1.5. Fig. S2 shows the STM images of naphthalene on the Au(111) surface obtained at a low coverage. As shown in Fig. S2(a), we found herringbone structures of the Au(111) surface and most molecules have adsorbed at the elbow sites of the herringbone structures and step edges, which are well known as preferential adsorption sites on the Au(111) surface.^{S8-S11} A proposed molecular arrangement model for naphthalene on the Au(111) surface at low coverages is shown in Scheme S2(a). The molecular size is approximately 9 Å, as shown in Fig. S2(b). We suggest that the adsorption of naphthalene is affected by the surface, because there are no strong interactions between naphthalene molecules. As a result, naphthalene molecule is unable to build self-assembled naphthalene structures at low coverages.

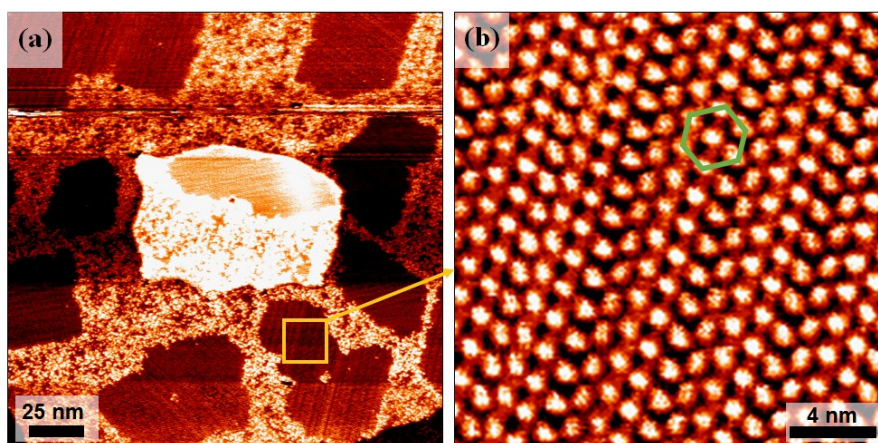


Fig. S3 High coverage filled-state STM images of naphthalene on the Au(111) surface at 150 K: (a) $198.0 \times 198.0 \text{ nm}^2$, $V_s = -2.0 \text{ V}$, $I_t = 0.1 \text{ nA}$, (b) magnified image of (a), $15.0 \times 15.0 \text{ nm}^2$, $V_s = -2.0 \text{ V}$, $I_t = 0.1 \text{ nA}$.

We then further increased the naphthalene deposition coverage, which results in the formation of well-ordered 1D and 2D self-assembled structures,^{S8} as evident in Fig. 4. However, as shown in Fig. S3(a), this well-ordered structure is sparse. Therefore, we suggest that naphthalene is less interactive than **1** between molecules. Fig. S3(b) shows a magnified image, which demonstrates that in contrast to **1**, naphthalene self-assembles in a closed packed structure with a hexagonal lattice. As is well known, a hexagonal closed packing structure is denser than a square closed packing structure. This difference is due to the difference for the existence of functional groups and molecular sizes between **1** and naphthalene. A proposed molecular arrangement model of naphthalene on the Au(111) surface at high coverages is shown in Scheme S2(b). This structure is induced by parallel displaced π - π stacking interactions of naphthalene molecules.^{S12} Naphthalene can form a long-range ordered self-assembled structure at high coverages, but does not form self-

assembled structures at low coverages, whereas **1** can form a self-assembled structure even at low coverages.

HRPES of Naphthalene on the Au(111) Surface

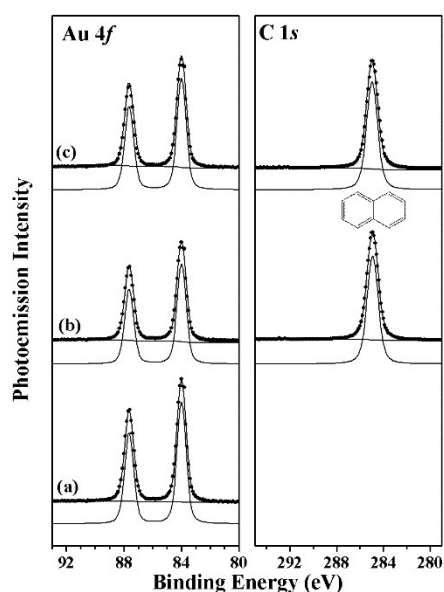
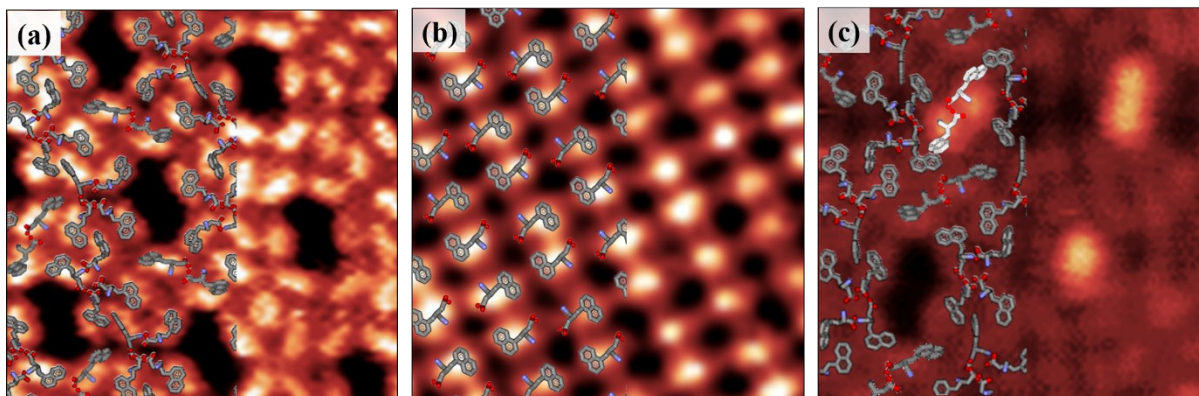


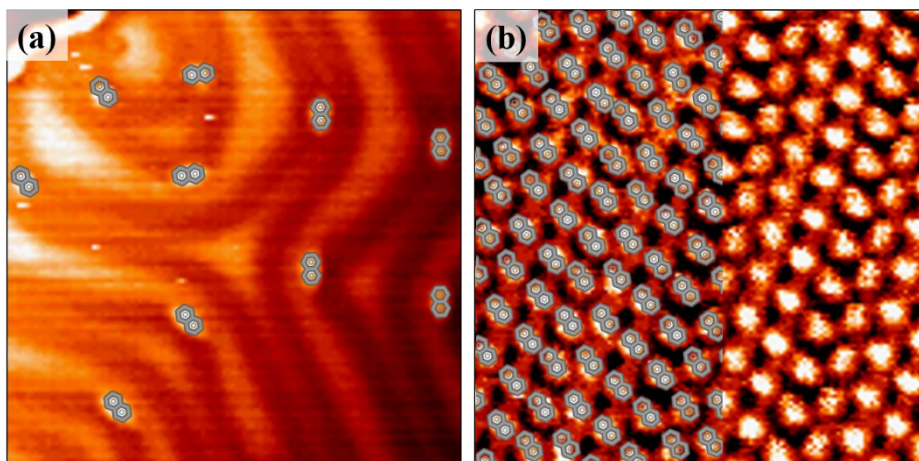
Fig. S4 The coverage-dependent core-level photoemission spectra of naphthalene on the Au(111) surface at a low temperature.

In addition, we characterized naphthalene on the Au(111) surface by using HRPES, and we obtained Au 4*f* core-level spectra and C 1*s* core-level spectra as the coverage of naphthalene increases. As for naphthalene, Au 4*f* (83.95 eV) does not change when the coverage is increased (as shown in Fig. S4(a), (b), and (c)). We also acquired the C 1*s* spectrum and found only one carbon bonding feature (284.21 eV, aromatic carbon), so naphthalene molecules adsorb onto the Au(111) surface without bond breaking.

Proposed Structural Models for **1** and Naphthalene on the Au(111) surface



Scheme S1. Proposed structural models for **1**. (a) low coverage and (b), (c) high coverage of **1** on the Au(111) surface. In Scheme S1(c), two layers of molecules are observed in the pores. Dark molecules belong to bottom layer and bright molecules to the top layer.



Scheme S2. Proposed model of (a) the low coverage and (b) the high coverage structures of naphthalene on the Au(111) surface.

References

- S1 T. Ok, A. Jeon, J. Lee, J.-H. Lim, C. S. Hong and H.-S. Lee, *J. Org. Chem.*, 2007, **72**, 7390-7393.
- S2 C. Lee, W. Yang and R. G. Parr, *Phys. Rev. B*, 1988, **37**, 785-789.
- S3 A. D. Becke, *Phys. Rev. A*, 1988, **38**, 3098-3100.
- S4 W. Kohn, A. D. Becke and R. G. Parr, *J. Phys. Chem.*, 1996, **100**, 12974-12980.
- S5 F. Schreier, *J. Quant. Spectrosc. Radiant. Transfer.*, 1992, **48**, 743-762.
- S6 V. Humblot, F. Tielens, N. B. Luque, H. Hampartsoumian, C. Methivier and C.-M. Pradier, *Langmuir*, 2014, **30**, 203–212.
- S7 S. Yang, Y. Park, J. W. Kim and H. Lee, *J. Phys. Chem. C*, 2011, **115**, 19287–19292.
- S8 Y. Wang, Y. Ye and K. Wu, *J. Phys. Chem. B*, 2006, **110**, 17960-17965.
- S9 J. A. Meyer, I. D. Baikie, E. Kopatzki and R. J. Behm, *Surf. Sci.*, 1996, **365**, L647-L651.
- S10 X. Zhang, L. Tang and Q. Guo, *J. Phys. Chem. C*, 2010, **114**, 6433–6439.
- S11 B. K. Min, X. Deng, D. Pinnaduwaage, R. Schalek and C. M. Friend, *Phys. Rev. B*, 2005, **72**, 121410(R).
- S12 C. Vaz-Domínguez, M. Escudero-Escribano, A. Cuesta, F. Prieto-Dapena, C. Cerrillos and M. Rueda, *Electrochem. Commun.*, 2013, **35**, 61-64.